

# WOBBLING NUCLEUS I

R. POENARU<sup>1,2,a</sup>, A. A. RADUTA<sup>2,3,b</sup>

<sup>1</sup>Doctoral School of Physics, University of Bucharest, Bucharest, Romania  
*E-mail*<sup>a</sup>: robert.poenaru@drd.unibuc.ro

<sup>2</sup>Department of Theoretical Physics - *Horia Hulubei* National Institute for Physics and Nuclear Engineering, Măgurele-Bucharest, Romania  
*E-mail*<sup>b</sup>: raduta@nipne.ro (corresponding author)

<sup>3</sup>Academy of Romanian Scientists, Bucharest, Romania

Received: April 15, 2021 (RJP v2.0 r2018a)

*Abstract.* Abstract 1.

*Key words:* Nuclear Structure, Triaxial Nuclei, Wobbling Motion, Parity Symmetry, Signature Partners, Strong Deformation.

*PACS:* 01.30.-y, 01.30.Ww, 01.30.Xx, 99.00.Bogus

## 1. INTRODUCTION

The experimental observations regarding wobbling motion have been quite rare, even though this kind of collective motion has been theoretically predicted almost 50 years ago by Bohr and Mottelson [?] when they were investigating the rotational modes of a triaxial nucleus employing a Triaxial Rotor Model (TRM). Therein, it was shown that for a triaxial rotor, the main rotational motion is around the axis with the largest moment of inertia (MOI), as it is energetically the most favorable. This mode is quantum-mechanically disturbed by the rotation around the other two axes, since rotation around any of the three principal axes of the system are possible, due to the anisotropy between the MOIs (that is  $\mathcal{I}_1 \neq \mathcal{I}_2 \neq \mathcal{I}_3$ ). Naturally, the description of the energy spectra and electromagnetic transitions between the rotational states of these wobbling nuclei (also known as *wobblers*) are considered to be the main characteristics that are put to the test by a theoretical investigation. The overall agreement between experimental results and the theoretically obtained data serves as an indicator for the quality of the model used to describe the wobbling picture.

The present work aims at extending the knowledge of the wobbling characteristics in an even-odd nucleus, which will be done by studying the energy spectrum of <sup>163</sup>Lu in a semi-classical approach, where the rotational states are described through a set of classical equations. In contradistinction with previous work, [?], in this formalism, all four wobbling bands are described by the same *core-quasiparticle*

34 *alignment*, making thus the description of the wobbling motion consistent. A re-  
 35 marking feature for the current research is the introduction of the concept of *parity*  
 36 *partner bands* - concerning the states from  $TSD_2$  and  $TSD_4$  bands - which will be  
 37 discussed throughout the paper.

## 2. RE-INTERPRETATION OF THE WOBBLING BANDS IN $^{163}\text{Lu}$

38 Considered the *best wobbler* to date,  $^{163}\text{Lu}$  has a rich wobbling spectrum [?  
 39 ? ], with no less than four such wobbling bands: one yrast -  $TSD_1$ , (zero-phonon  
 40 wobbling number  $n_w = 0$ ), and three excited wobbling bands -  $TSD_{2,3,4}$  (with their  
 41 corresponding wobbling phonon numbers  $n_w = 1, 2, 3$ ). The name TSD comes from  
 42 Triaxial Strongly Deformed bands. The triaxial bands emerge due to the coupling of  
 43 an odd- $\vec{j}$  nucleon with an even-even triaxial core. Thus, for  $^{163}\text{Lu}$ , it is the intruder  
 44  $\pi(i_{13/2})$  that couples to the triaxial core [? ? ? ], driving the nuclear system up to  
 45 large deformation, and stabilizing the deformed structure. Indeed, a triaxial shape  
 46 with deformation parameters  $(\epsilon_2, \gamma) \approx (0.38, +20^\circ)$  is assumed to be in agreement  
 47 with the observed data, based on calculations using the Ultimate Cranker Code [? ]  
 48 for the potential energy surface (PES).

49 In terms of the experimental evidence which should be pointing out wobbling  
 50 nature for the four TSD bands belonging to  $^{163}\text{Lu}$ , the large transition quadrupole  
 51 moment  $Q_t \approx 10 b$  [? ], the predominantly  $E2$  character of the transitions linking  
 52 adjacent bands ( $I \rightarrow I - 1$ ), a large  $E2/M1$  mixing ratio  $\delta > 1$  for the transitions  
 53 linking the yrare ( $n_w = 1$ ) and yrast ( $n_w = 0$ ) bands are all clear fingerprints of wob-  
 54 bbling nature. For a set of results concerning these quantities (both theoretical and  
 55 experimental), see Ref. [? ], and the references cited therein. Another quantity that  
 56 indicates strong deformation with wobbling character is the relative rigid rotor en-  
 57 ergy, and for this isotope, calculations show that all four bands have similar behavior  
 58 with respect to this value (see Figures 3 and 4 from Ref. [? ]).

59 A fully semi-classical approach for the description of the wobbling spectrum  
 60 of  $^{163}\text{Lu}$  was by Raduta et. al. [? ]. A diagram that shows the workflow involved in  
 61 W1 can be seen in Figure ?? from the Appendix. Also, a comparison with previous  
 62 calculations can be seen in Figure 21 from Ref. [? ].

### 2.1. W2 - SIGNATURE PARTNER BANDS + PARITY PARTNER BANDS

63 The main question which can be asked regarding the formalism W1 that was de-  
 64 scribed in ?? is whether it is possible to obtain a *unified* description for all four bands  
 65 in  $^{163}\text{Lu}$  concerning the coupling scheme. In other words, it is worth investigating  
 66 the possibility of having a unique single-particle state  $j$  that is coupled to a core of  
 67 positive parity for the bands  $TSD_{1,2,3}$  and a core of negative parity for  $TSD_4$ .

Fortunately, the answer is positive: starting from the semi-classical formalism of W1, one can properly adjust the coupling scheme, making sure that the entire numerical recipe used for obtaining the energy spectrum of  $^{163}\text{Lu}$  remains consistent with the experimental results.

Regarding the unique single-particle that couples to the triaxial core, it is natural to pick the  $i_{13/2}$  proton (that is  $j_1$  from W1). The reasoning behind this choice has to do with the microscopic calculations [? ? ?] that showed stable triaxial structures in the  $^{163}\text{Lu}$  potential energy surface when the triaxial core couples with a highly aligned  $j$ -shell particle, indicating the  $\pi(i_{13/2})$  proton. Keep in mind that a highly aligned  $j$ -nucleon will *prefer* to keep a certain triaxial deformation when coupled to a core [? ? ?] (in the sense that the triaxiality parameter  $\gamma$  will have a certain value based on the orbital of the odd nucleon), and using microscopic calculations following the Ultimate Cranker code, it has been shown that a value of  $\gamma \approx +20^\circ$  is preferred by the odd  $\pi(i_{13/2})$  nucleon.

By taking  $j = j_1$  as the sole intruder that couples to a positive core and also a negative core, the sequences with even/odd integer spins for the core do not change. In fact, the coupling schemes can be readily obtained:

1. Coupling  $C'_1$ : the odd  $j_1$  proton aligns with the core of even-integer spin sequence  $R_1 = 0, 2, 4, \dots$ , with a parity of the  $R_1$  core that is positive  $\pi(R_1) = +1$ .
2. Coupling  $C'_2$ : the odd  $j_1$  proton aligns with the core of even-integer spin sequence  $R_2^+ = 1, 3, 5, \dots$ , with a parity of the  $R_2^+$  core that is positive  $\pi(R_2^+) = +1$ .
3. Coupling  $C'_3$ : the odd  $j_1$  proton aligns with the core with an odd-integer spin sequence  $R_2^- = 1, 3, 5, \dots$ , which has negative parity  $\pi(R_2^-) = -1$ .

From the three schemes defined above, it is clear that  $C'_1$  corresponds to the yrast  $TSD_1$ ,  $C'_2$  to the ground state  $TSD_2$ , and finally  $C'_3$  to the ground state  $TSD_4$ . Obviously, the odd valence nucleon  $j_1$  has a positive parity  $\pi_{j_1} = +1$ . There has not been attributed a coupling scheme for  $TSD_3$ , since this band still remains as the one-wobbling phonon excitation that is built on top of  $TSD_2$  with the action of a phonon operator which will be characterized later on.

The last step in searching for a unified coupling scheme in  $^{163}\text{Lu}$  is to establish a possible relationship between the four bands. As per the calculations involved in W1, it was proven that signature is a good quantum number and indeed, a sign that  $TSD_1$  and  $TSD_2$  are signature partners emerged. Their overall similar properties and spin difference enforce this argument. Furthermore, in this new W2 approach, the difference in parity between the  $TSD_2$  and  $TSD_4$  but the same angular momentum sequence of their corresponding triaxial core  $R_2^+$  and  $R_2^-$  strongly suggest that the two bands are *Parity Partner Bands*: two rotational sequences with energy states characterized by opposite parity, increasing energy that follows a trend  $\propto I(I+1)$ ,

and a spin difference  $\Delta I = 2$  between states belonging to the same band. In the following section, calculations which will show that parity is indeed a good quantum number for the triaxial rotor + odd-particle system will be provided. For what it is worth mentioning now is that the concept of parity partners between  $TSD_2$  and  $TSD_4$  emerge from the idea that a stable strongly deformed structure is achieved from a single quasiparticle that moves in a quadrupole mean-field generated by a triaxial even-even core. However, there is a splitting in two different cases of coupling mechanisms, namely  $C'_2/C'_3$  depending on the alignment of the high- $j$ -shell particle with a core of positive/negative parity.

Similar structures with alternating positive-negative parity bands have been also reported in other nuclei such as  $^{40}\text{Ca}$  [? ], or some heavier isotopes like  $^{218}\text{Fr}$  [? ]. In fact, a unified description of states with positive and negative parity in odd-mass nuclei was made over the last decade [? ? ], although therein, a quadrupole-octupole term was introduced within the particle-core Hamiltonian to describe this feature. A diagram which shows the workflow involved in W2 can be seen in the Figure ?? from the Appendix ??.

### 3. THEORETICAL FORMALISM

In this section, a description of the framework used for obtaining the wobbling spectrum of  $^{163}\text{Lu}$  is made. As stated in the previous section, the system is described with a similar Hamiltonian used in W1, namely the Hamiltonian for the triaxial PRM.

$$H = H_{\text{core}} + H_{\text{s.p.}} . \quad (1)$$

The Hamiltonian from Eq. 1 describes a system in which an odd  $j$  particle interacts with a triaxial even-even core, i.e., the odd nucleon is moving in a quadrupole deformed mean-field that is generated by the core. As such, the first term in the Hamiltonian  $H_{\text{core}}$  describes the motion of a triaxial core, while the second term  $H_{\text{s.p.}}$  represents the single-particle potential characterizing the valence proton.

Indeed, the core Hamiltonian is given by:

$$H_{\text{core}} = \sum_{i=1,2,3} \frac{1}{2\mathcal{I}_i} (I_i - j_i)^2 , \quad (2)$$

where the core angular momentum is  $\vec{R} = \vec{I} - \vec{j}$  and the terms  $\mathcal{I}_i$  represent the moments of inertia for a triaxial ellipsoid, along the principal axes. These three moments of inertia will be considered as free parameters in the present calculations, but, compared to the work W1, a unique set of MOIs will be attributed to the four bands, since the triaxial core will create an alignment with a unique particle, that is  $j_1$ . Because of this, there is no option for their nature (i.e., rigid or hydrodynamic).

The single-particle Hamiltonian from Eq. 1 is derived from the well-known

Nilsson potential [? ? ]:

$$h(\beta_2, \gamma) = C \left\{ \cos \gamma Y_{20}(\theta, \varphi) + \frac{\sin \gamma}{\sqrt{2}} [Y_{22}(\theta, \varphi) + Y_{2-2}(\theta, \varphi)] \right\}, \quad (3)$$

where the coupling parameter  $C$  causes the level splitting in the deformed field and it is proportional to the quadrupole deformation  $\beta_2$ . The potential  $h$  from Eq. 3 is written in terms of the quadrupole deformation and triaxiality parameter that play the role of deformation parameters within a triaxial system  $(\beta_2, \gamma)$ . Its expression using the coupling parameter  $C$  is widely used when working with a particle-rotor-model [? ? ? ]. In the present this case, the change  $h(\beta_2, \gamma) \rightarrow H_{\text{s.p.}}$  is done by applying the Wigner-Eckart theorem for the single- $j$  particle, and the following expression for  $H_{\text{s.p.}}$  will be obtained:

$$H_{\text{s.p.}} = \frac{V}{j(j+1)} \left[ \cos \gamma (3j_3^2 - \vec{j}^2) - \sqrt{3} \sin \gamma (j_1^2 - j_2^2) \right] + \epsilon_j. \quad (4)$$

133 This term describes the motion of an odd particle with angular momentum  $j$  in  
134 a mean-field generated by a triaxial core, with a potential strength  $V$  characterized by  
135 the quadrupole deformation ( $V \propto \beta_2$ ). In fact, the single-particle potential strength  
136  $V$  will be considered as the fourth free parameter within the calculations and its  
137 behavior will dictate the coupling of the  $j$  particle with all four TSD bands. The  
138 term  $\epsilon_j$  from Eq. 4 represents the single-particle energy that corresponds to the odd  
139  $j$  proton from the  $i$ -orbital. One should not mix up the  $j_1$  proton notation used  
140 throughout the paper with the components of the single-particle angular momentum  
141 from Eq. 4.

142 Regarding the triaxial deformation  $\gamma$  which enters in Eq. 4, its value will be  
143 considered as another free parameter of the current problem. In other words, having  
144  $V$  and  $\gamma$  as free parameters means that the system will be described by its deformation  
145 parameters which will be obtained through a fitting procedure, keeping an agreement  
146 with the experimental data regarding the excitation energies of the rotational states  
147 belonging to  $TSD_{1,2,3,4}$ .

From Eqs. 2 and 4, the free parameter set can be obtained, hereafter denoted by  $\mathcal{P}$ . It comprises three moments of inertia, the single-particle potential strength, and the triaxial deformation. As such,  $\mathcal{P}$  can be written as:

$$\mathcal{P} = [\mathcal{I}_1, \mathcal{I}_2, \mathcal{I}_3, V, \gamma]. \quad (5)$$

Solving the problem of W2 is equivalent to finding the eigenvalues of  $H$  given in Eq. 1. In a similar approach as in W1, the eigenvalues of interest are obtained on the base of a semi-classical approach. Thus, the first step is to perform a de-quantization

procedure on  $H$  through a TDVE [? ? ? ]:

$$\delta \int_0^t \langle \Psi_{IJM} | H - i \frac{\partial}{\partial t'} | \Psi_{IJM} \rangle dt' = 0 . \quad (6)$$

Working within a semi-classical approach allows one to keep close contact with the system's dynamics in terms of equations of motion for the generalized coordinates. The trial function from Eq. 6 is carefully chosen as a product of two basis states comprising the states with total angular momentum  $I$  and  $j$ , respectively:

$$|\Psi_{IJM}\rangle = \mathbf{N} e^{z\hat{I}_-} e^{s\hat{j}_-} |IMI\rangle |jj\rangle , \quad (7)$$

148 where the operators  $\hat{I}_-$  and  $\hat{j}_-$  denote the lowering operators for the intrinsic angular  
149 momenta  $\vec{I}$  and  $\vec{j}$ , respectively, and  $\mathbf{N}$  plays the role of the normalization constant.  
150 One must remark the fact that the states  $|IMI\rangle$  and  $|jj\rangle$  from Eq. 7 are extremal  
151 states for the operators  $(\hat{I}^2, \hat{I}_3)$  and  $(\hat{j}^2, \hat{j}_3)$ , respectively, and they correspond to  
152 the maximally allowed states for a given set of angular momenta  $I$  and  $j$ . As an  
153 observation, the trial function is an admixture of components of definite  $K$ , which is  
154 consistent with the fact that for a triaxial nucleus,  $K$  is not a good quantum number.

The variables  $z$  and  $s$  from Eq. 7 are complex functions of time, and they play the role of classical coordinates in the phase spaces that describe the motion of the core and the odd particle:

$$z = \rho e^{i\varphi} , \quad s = f e^{i\psi} . \quad (8)$$

In order to obtain a set of classical equations in a Hamilton Canonical form, a new pair of variables are introduced:

$$r = \frac{2I}{1 + \rho^2} , \quad t = \frac{2j}{1 + f^2} , \quad (9)$$

where  $r \in [0, 2I]$  and  $t \in [0, 2j]$ . Thus the equations of motion acquire the form:

$$\begin{aligned} \frac{\partial \mathcal{H}}{\partial r} &= \dot{\varphi} ; \quad \frac{\partial \mathcal{H}}{\partial \varphi} = -\dot{r} , \\ \frac{\partial \mathcal{H}}{\partial t} &= \dot{\psi} ; \quad \frac{\partial \mathcal{H}}{\partial \psi} = -\dot{t} . \end{aligned} \quad (10)$$

The function  $\mathcal{H}$  denotes the average of the Hamiltonian operator  $H$  (Eq. 1) with the trial function  $|\Psi_{IJM}\rangle$  given in Eq. 7, and it plays the role of classical energy:

$$\mathcal{H}(\varphi, r; \psi, t) = \langle \Psi_{IJM} | H | \Psi_{IJM} \rangle , \quad (11)$$

155 Starting from the equations of motion given in Eq. 10, one can observe that the  
156 function  $\mathcal{H}$  is a constant of motion, that is  $\dot{\mathcal{H}} \equiv 0$ . This equation will define a surface,  
157 a so-called equi-energy surface  $\mathcal{H} = \text{const}$ . It is worth mentioning the fact that such  
158 equality holds since the entire set of equations of motion emerged from a variational

principle. The sign of the Hessian associated to this classical function will indicate its stationary points. Among them, some are minima. The critical points which are of interest for the present study are those obtained when the following ordering for the three moments of inertia holds:  $\mathcal{I}_1 > \mathcal{I}_2 > \mathcal{I}_3$ . There is no restriction on  $\gamma$ .

With a linearization procedure for the equations of motion around the minimum point of  $\mathcal{H}$ , a dispersion equation will be obtained:

$$\Omega^4 + B\Omega^2 + C = 0. \quad (12)$$

The above equation describes a harmonic type of motion for the nuclear system, with the solutions to this algebraic equation as the *wobbling frequencies*  $\Omega$ . The terms  $B$  and  $C$  are functions of total angular momentum  $I$ , single-particle a.m.  $j$ , inertial parameters  $A_k = 1/(2\mathcal{I}_k)$ ,  $k = 1, 2, 3$ , single-particle potential strength  $V$ , and triaxiality parameter  $\gamma$ . The  $B$  term from Eq. 12 has the expression [? ]:

$$-B = [(2I - 1)(A_3 - A_1) + 2jA_1][(2I - 1)(A_2 - A_1) + 2jA_1] + 8A_2A_3Ij + T_B^1 T_B^2, \quad (13)$$

where the terms  $T_B^1$  and  $T_B^2$  are defined defined as:

$$\begin{aligned} T_B^1 &= \left[ (2j - 1)(A_3 - A_1) + 2IA_1 + V \frac{2j - 1}{j(j + 1)} \sqrt{3}(\sqrt{3} \cos \gamma + \sin \gamma) \right], \\ T_B^2 &= \left[ (2j - 1)(A_2 - A_1) + 2IA_1 + V \frac{2j - 1}{j(j + 1)} 2\sqrt{3} \sin \gamma \right]. \end{aligned} \quad (14)$$

Accordingly, the  $C$  term from Eq. 12 has the expression [? ]:

$$\begin{aligned} C &= \{ [(2I - 1)(A_3 - A_1) + 2jA_1] T_C^1 - 4IjA_3^2 \} \\ &\quad \times \{ [(2I - 1)(A_2 - A_1) + 2jA_1] T_C^2 - 4IjA_2^2 \}, \end{aligned} \quad (15)$$

where the terms  $T_C^1$  and  $T_C^2$  are defined defined as:

$$\begin{aligned} T_C^1 &= \left[ (2j - 1)(A_3 - A_1) + 2IA_1 + V \frac{2j - 1}{j(j + 1)} \sqrt{3}(\sqrt{3} \cos \gamma + \sin \gamma) \right], \\ T_C^2 &= \left[ (2j - 1)(A_2 - A_1) + 2IA_1 + V \frac{2j - 1}{j(j + 1)} 2\sqrt{3} \sin \gamma \right]. \end{aligned} \quad (16)$$

It can be seen that the terms which enter in  $B$  and  $C$ , namely  $(T_B^1, T_B^2)$  from Eq. 14 and  $(T_C^1, T_C^2)$  from Eq. 16 correspond to the quadrupole deformation that causes the single-particle to move in the mean-field of the triaxial core. The terms also define the triaxiality that the nucleus achieves once the odd proton couples to the triaxial core, driving the system up to a large (and stable) deformation.

Going back to Eq. 12, under the restrictions for the MOIs defined above, the dispersion equation admits two real and positive solutions (hereafter denoted with

$\Omega_1^I$  and  $\Omega_2^I$ , where  $\Omega_1^I < \Omega_2^I$ ) defined for  $j_1 = i_{13/2}$ , given by:

$$\Omega_{1,2}^I = \sqrt{\frac{1}{2}(-B \mp (B^2 - 4C)^{1/2})}. \quad (17)$$

These two solutions are interpreted as *wobbling frequencies* associated with the motion of the core, and the motion of the odd-particle respectively. As such, each wobbling frequency has an associated wobbling-phonon number:

$$\Omega_1^I \rightarrow n_{w_1}; \Omega_2^I \rightarrow n_{w_2}. \quad (18)$$

Now the analytical expressions for the four TSD bands in  $^{163}\text{Lu}$  are readily obtained:

$$\begin{aligned} E_{\text{TSD1}}^I &= \epsilon_j + \mathcal{H}_{\min}^{(I,j)} + \mathcal{F}_{00}^I, \quad I = 13/2, 17/2, 21/2 \dots \\ E_{\text{TSD2}}^I &= \epsilon_j^1 + \mathcal{H}_{\min}^{(I,j)} + \mathcal{F}_{00}^I, \quad I = 27/2, 31/2, 35/2 \dots \\ E_{\text{TSD3}}^I &= \epsilon_j + \mathcal{H}_{\min}^{(I-1,j)} + \mathcal{F}_{10}^{I-1}, \quad I = 33/2, 37/2, 41/2 \dots \\ E_{\text{TSD4}}^I &= \epsilon_j^2 + \mathcal{H}_{\min}^{(I,j)} + \mathcal{F}_{00}^I, \quad I = 47/2, 51/2, 55/2 \dots, \end{aligned} \quad (19)$$

where  $\mathcal{F}_{n_{w_1} n_{w_2}}^I$  is a function of the wobbling frequencies:

$$\mathcal{F}_{n_{w_1} n_{w_2}}^I = \Omega_1^I \left( n_{w_1} + \frac{1}{2} \right) + \Omega_2^I \left( n_{w_2} + \frac{1}{2} \right), \quad (20)$$

and  $\mathcal{H}_{\min}^{(I,j)}$  is the classical energy evaluated in its minimal point. For the present case, its analytical expression is given by the following equation:

$$\mathcal{H}_{\min}^{(I,j)} = (A_2 + A_3) \frac{I+j}{2} + A_1(I-j)^2 - V \frac{2j-1}{j+1} \sin \left( \gamma + \frac{\pi}{6} \right). \quad (21)$$

A few aspects regarding the energy spectrum defined in Eq. 19 are worth mentioning. To each band, there is a specific energy  $\epsilon_j$  associated with the single-particle state. In this case, the odd-proton  $j_1 = 13/2$  from the  $i$ -orbital is the one that couples to the triaxial core. However, for the bands  $TSD_2$  and  $TSD_4$ , a different re-normalization of  $\epsilon_j$  is considered, since  $TSD_2$  is the unfavored signature partner of  $TSD_1$ , and  $TSD_4$  is the negative parity partner of  $TSD_2$  within the band structure. These quantities will shift the overall energy states belonging to the two bands, each by a different amount. As a result, both  $\epsilon_j^1$  and  $\epsilon_j^2$  will be adjusted throughout the numerical calculations such that the energy spectrum is best reproduced. Another aspect concerns the band  $TSD_3$ ; since this is the only excited wobbling band within the family, its configuration is built on top of  $TSD_2$ , with the action of a single phonon ( $n_{w_1} = 1$ ) operator. Consequently, an energy state  $I$  belonging to  $TSD_3$  is obtained from a state  $I - 1$  from  $TSD_2$ . In Table 1, the rest of the wobbling phonon numbers are mentioned, with the parity, signature, and coupling scheme for each band in



Band	$n_{w_1}$	$n_{w_2}$	$\pi$	$\alpha$	Coupling scheme
$TSD_1$	0	0	+1	+1/2	$C'_1$
$TSD_2$	0	0	+1	-1/2	$C'_2$
$TSD_3$	1	0	+1	+1/2	Built on top of $TSD_2$
$TSD_4$	0	0	-1	-1/2	$C'_3$

Table 1

The wobbling phonon numbers, parities, signatures, and coupling schemes assigned to each triaxial band in  $^{163}\text{Lu}$ , within the W2 model. The three coupling schemes were defined in Section 2.1.

particular.

### 3.1. PARITY QUANTUM NUMBER FOR THE WAVE-FUNCTION

In W1 it was shown that signature emerges from the calculations on the total wave-function as a good quantum number for this triaxial system. This is why in [?] the bands  $TSD_1$  and  $TSD_2$  appeared as Signature Partner Bands (SPB). In W2, such property still stands.

Since the backbone of the current work started from the need for a single odd-particle that couples to a triaxial core in  $^{163}\text{Lu}$ , one has to look at the band  $TSD_4$  (which was interpreted as having a different nucleon:  $j_2$  with  $j = 9/2$  from the  $h$ -orbital), and see if its differentiating properties can be linked to *main group* of bands (namely  $TSD_{1,2,3}$ ). Indeed, from the experimental measurements regarding spin and parity assignment [?], it turns out that the parity of the rotational states is negative. Therefore, a forensic analysis on this quantum property should be considered as the necessary ingredient in a unified description of all four bands.

The parity operator is defined as a product of the complex conjugation operation and a rotation of angle  $\pi$  around the 2-axis:  $P = e^{-i\pi\hat{I}_2}C$ . The total parity operator is the product of an operator corresponding to the core and one corresponding to the single-particle:

$$\mathcal{P}_T = P_{\text{core}}P_{\text{s.p.}} . \quad (22)$$

Acting with the total parity operator defined above, on the trial function  $\Psi$  associated, the following result is obtained:

$$\mathcal{P}_T\Psi(r, \varphi; t, \psi) = \Psi(r, \varphi + \pi; t, \psi + \pi) \stackrel{\text{not.}}{=} \bar{\Psi}. \quad (23)$$

The classical energy function  $\mathcal{H}$  has an invariance property at changing the angles with  $\pi$ :

$$\mathcal{H}(r, \varphi; t, \psi) = \mathcal{H}(r, \varphi + \pi; t, \psi + \pi) . \quad (24)$$

From Eqs. 23 and 24, it can be concluded that the wave-function describing the

Band	$n_s$	$\vec{j}$	$\vec{R}$ - Sequence	$\vec{I}$ - Sequence	Coupling scheme
$TSD_1$	21	$j_1$	$R_1 = 0, 2, 4, \dots$	$13/2, 17/2, 21/2, \dots$	$C'_1$
$TSD_2$	17	$j_1$	$R_2^+ = 1^+, 3^+, 5^+, \dots$	$27/2, 31/2, 35/2, \dots$	$C'_2$
$TSD_3$	14	$j_1$	1-phonon excitation	$33/2, 37/2, 41/2, \dots$	1-phonon excitation
$TSD_4$	11	$j_1$	$R_2^- = 1^-, 3^-, 5^-, \dots$	$47/2, 51/2, 55/2, \dots$	$C'_3$

Table 2

The number of energy states  $n_s$  within each wobbling band, the a.m. of the proton  $\vec{j}$ , the core's a.m.  $\vec{R}$ , the nucleus' a.m.  $\vec{I}$ , and the corresponding coupling scheme that was established according to the W2 model. The single-particle is the  $j_1 = (i_{13/2})$  proton.

triaxial system  $\Psi$  and its image through  $\mathcal{P}_T$ ,  $\bar{\Psi}$ , are two linearly dependent functions which differ only by a multiplicative constant  $p$ , with  $|p| = 1$ . Thus,  $p$  can either be -1 or +1, such that:

$$\bar{\Psi} = \pm \Psi(r, \varphi; t, \psi) . \quad (25)$$

195 The above result concludes the parity analysis for the wave-function, showing  
 196 that the triaxial rotor admits eigenfunctions of negative parity. Therefore, a single  
 197 wave-function characterized by the coupling of a triaxial core to the odd proton  $i_{13/2}$   
 198 is describing both positive parity states ( $\in TSD_{1,2,3}$ ) as well as negative parity states  
 199 ( $\in TSD_4$ ). This analysis, together with the fact that  $TSD_2$  and  $TSD_4$  have the same  
 200 a.m. sequences (although  $TSD_2$  has more states with low spin than  $TSD_4$ ) suggest  
 201 the fact that these two bands might be Parity Partners.

#### 4. NUMERICAL RESULTS

As a first step, the results concerning the excited spectrum of the four TSD bands will be presented. Regarding the wobbling spectrum of  $^{163}\text{Lu}$ , its analytical formulation was given in Eq. 19. As mentioned, those energies are parametrized in terms of  $\mathcal{P}$ , which is the set of free parameters to be determined. Indeed, one can find  $\mathcal{P}$  by minimizing the  $\chi^2$  function:

$$\chi^2 = \frac{1}{N_T} \sum_i \frac{(E_{\text{exp}}^{(i)} - E_{\text{th}}^{(i)})^2}{E_{\text{exp}}^{(i)}} , \quad (26)$$

202 where  $N_T$  represents the total number of states. Table 2 contains the number of states  
 203 within each band, with the spin sequences for the core ( $\vec{R}$ ), the spin sequences for  
 204 the coupled system (that is the total angular momentum  $\vec{I}$ ), and the coupling schemes  
 205 specific to W2 formalism that is used in the current calculations.

206 The resulting values for  $\mathcal{P}$  are given in Table 3. This W2 method contrasts  
 207 the approach in W1, where a second minimization process was needed separately for

$\mathcal{I}_1 [\hbar^2/\text{MeV}]$	$\mathcal{I}_2 [\hbar^2/\text{MeV}]$	$\mathcal{I}_3 [\hbar^2/\text{MeV}]$	$\gamma [\text{deg.}]$	$V [\text{MeV}]$
72	15	7	22	2.1

Table 3

The parameter set  $\mathcal{P}$  that was determined by a fitting procedure of the excitation energies for  $^{163}\text{Lu}$ .

$TSD_4$ . The root mean square error provided by the obtained parameter set  $\mathcal{P}$  has a value of  $E_{\text{rms}} \approx 79$  keV. This result is much better than the one obtained with previous formalism W1 where an  $E_{\text{rms}} \approx 240$  keV was obtained [? ]. As a matter of fact, this is the first semi-classical formalism in the literature that achieves agreement with the experimental data with less than 100 keV for the entire wobbling spectrum of  $^{163}\text{Lu}$ . It is worth mentioning that the fitting procedure was done not for the absolute wobbling energies  $E_{\text{TSD}k}^I$ ,  $k = 1, 2, 3, 4$ , but for the *excitation energies* which are relative to the band-head  $I = 13/2^+$  from the first yrast band  $TSD_1$ . Comparison between the theoretical values obtained within the current formalism and the experimental data is shown in Figures 1 and 2. For the sake of completeness, the wobbling frequencies which enter in the expression of the  $\mathcal{F}_{n_{w1} n_{w2}}^I$  given by Eq. 20 are graphically represented as functions of total angular momentum  $I$  in Figure 3, for the fixed parameter set. It is remarkable the fact that the wobbling frequency  $\Omega_2^I$  is much larger than its partner, suggesting the fact the coupling effects caused by the highly aligned proton have a stronger influence in achieving a wobbling character for  $^{163}\text{Lu}$ , which is in line with the characteristics of a particle-rotor coupling. Another feature of these wobbling frequencies is their linear behavior with respect to the nuclear spin.

Concerning the single-particle energies from Eq. 19, namely  $\epsilon_j^1$  and  $\epsilon_j^2$  that emerge from the un-favored signature of  $TSD_2$  and negative parity of  $TSD_4$ , respectively, they induce a correction for the mean-field with the quantities  $\epsilon_j^1 - \epsilon_j = 0.3$  MeV and  $\epsilon_j^2 - \epsilon_j = 0.6$  MeV. Note that since the energy state  $I_{13/2} \in TSD_1$  (the band-head of  $TSD_1$ ) was subtracted from all bands, the single-particle energies for band 2 and 4 are adjusted accordingly.

The quantity  $\epsilon_j^1 - \epsilon_j$  is added to the second band due to the core, and such a splitting is caused by the fact that two distinct TDVE procedures were performed for the two partner bands  $TSD_{1,2}$ . The total signature splitting for the band-head and the terminus states of  $TSD_2$  are  $E_{TSD_2}^{27/2} - E_{TSD_2}^{25/2} = 0.492$  MeV and  $E_{TSD_2}^{91/2} - E_{TSD_2}^{89/2} = 0.936$  MeV which agrees with the estimate made by Jensen et. al. in [? ]. Although the signature splitting can be determined microscopically by using a deformed single-particle basis amended with a cranking constraint, for the present case it is obtained by applying the TDVE for each spin state and the correction corresponding to the single-particle energies (that is  $\epsilon_j^1$ ).

Another noteworthy aspect of the current formalism is the fact that the difference  $\delta_{42} = E_{\text{TSD}4}^I - E_{\text{TSD}2}^I$  for all the states has an almost constant value  $\delta_{42} \approx$

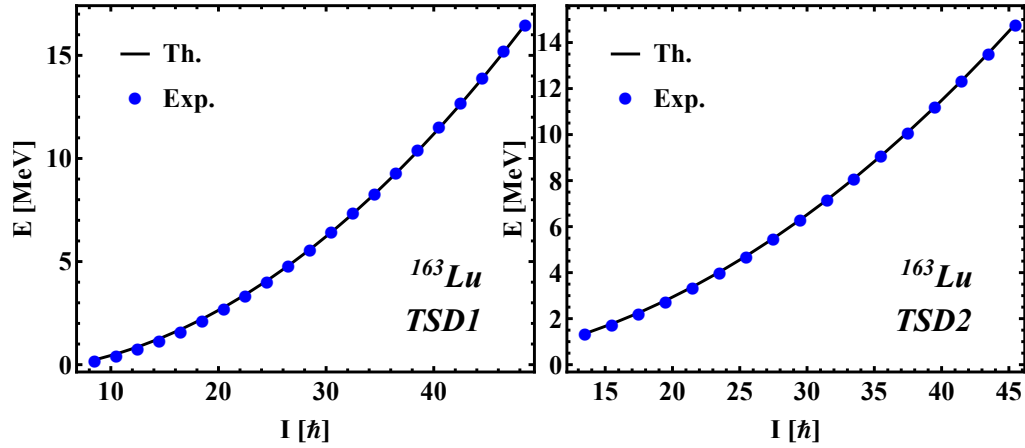


Fig. 1 – Comparison between theoretical and experimental excitation energies for the first two wobbling bands in  $^{163}\text{Lu}$  within the  $\mathbb{W}2$  model. The theoretical results are obtained with the parameters listed in Table 3. Experimental data is taken from [? ].

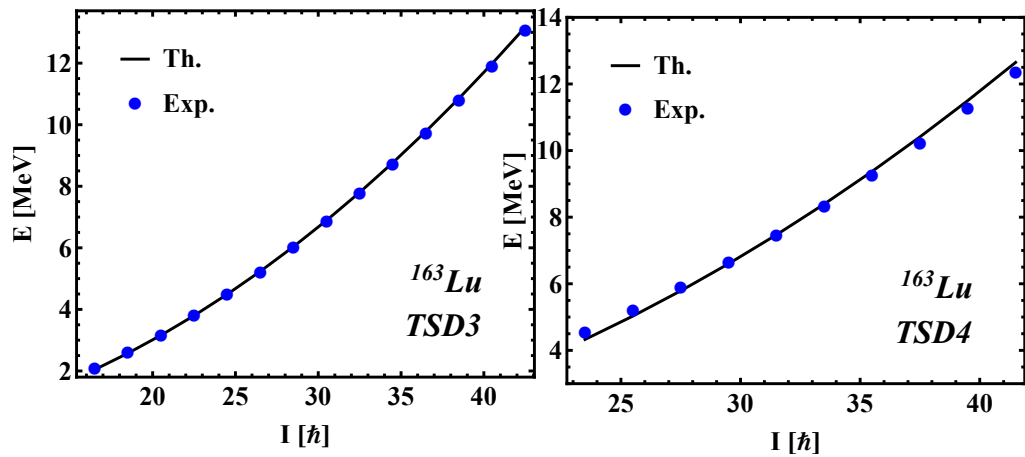


Fig. 2 – Comparison between theoretical and experimental excitation energies for third and fourth wobbling bands in  $^{163}\text{Lu}$  within the  $\mathbb{W}2$  model. The theoretical results are obtained with the parameters listed in Table 3. Experimental data is taken from [? ].

0.3 MeV. This suggests that the states of the same a.m. from  $TSD_2$  and  $TSD_4$  bands might emerge through the parity projection of a sole wave-function that does not have reflection symmetry. In the present case, this is caused by the fact that the wobbling frequency is parity-independent. It is interesting that the action of the parity operator on any rotational state within the angular momentum space will lead to the change of the angular momentum vector from  $\vec{I}$  to  $-\vec{I}$ . Due to this reason, the parity operator commutes with the initial Hamiltonian, and the eigenfunctions of  $H$  are characterized by either positive or negative parity (with states of different parities being degenerate). However, one can lift this degeneracy by using an additional linear in the expression  $H$ . Since in Eq. 1 such a linear term is missing, an *ad-hoc* correction of the mean-field with the amount 0.6 MeV for the states in  $TSD_4$  is necessary. As a result, the added shift simulates the breaking of parity symmetry. In contrast to this approach, using a microscopic formalism one starts with a single-particle basis generated by a mean-field without space reflection symmetry, followed by the calculation of the many-body wave-functions (being admixtures of both positive and negative parities). Restoration of the parity symmetry is achieved by selecting from all the wave-functions only the components with a definite parity (projecting the good parity), leading to a doublet structure of positive and negative parity states in the spectrum of  $H$ . Consequently, the bands  $TSD_2$  and  $TSD_4$  behave as a pair of parity partners, as defined in [? ? ?].

#### 4.1. INTERPRETATION OF THE PARAMETER SET $\mathcal{P}$

Performing the fitting procedure for the excitation energies of  $^{163}\text{Lu}$  will result in the moments of inertia  $\mathcal{I}_k$  that are given in Table 3, together with the single-particle potential strength  $V$ , and triaxiality parameter  $\gamma$ . Interpretation of their numerical values is mandatory in order to check whether the current formalism is valid or not.

Regarding the moments of inertia, it is clear that the axis of rotation for the energy ellipsoid is the 1-axis, as the largest MOI is  $\mathcal{I}_1$ , causing a maximal density distribution across this axis [? ]. The MOI ordering is  $\mathcal{I}_1 > \mathcal{I}_2 > \mathcal{I}_3$ , and compared with the results of the previous work W1, the current 1-axis MOI is bigger than both  $\mathcal{I}_1^{\text{TSD1,2,3}} = 63.2 \hbar^2/\text{MeV}$  and  $\mathcal{I}_1^{\text{TSD4}} = 67 \hbar^2/\text{MeV}$  (data taken from Table 1 in Ref. [? ]). This is expected, since here, the  $TSD_4$  band is obtained by the coupling of a higher aligned  $j$  particle, driving the system to an even larger deformation. One must remember that these are the *effective* MOIs of the entire system, that is the triaxial-rotor + odd-particle. No spin dependence has been inferred for the MOIs, so a possible change in the MOIs ordering with the increase in spin  $I$  cannot be studied within the current description. Furthermore, this formalism does not contain microscopic terms, so no presumptions on what causes the obtained MOI ordering can be stated. Although, by working with a quadrupole deformed mean-field, the

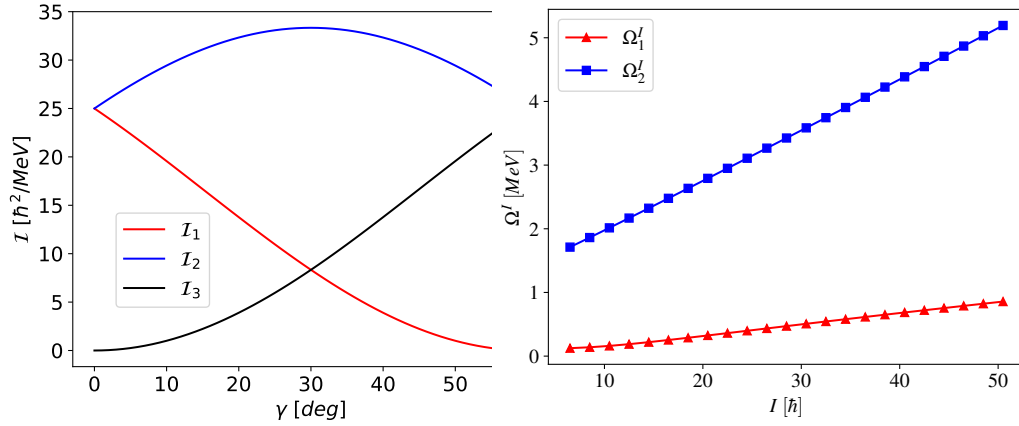


Fig. 3 – Left-side: The hydrodynamic moments of inertia [?] as function of the triaxiality parameter  $\gamma$ , for the positive interval  $\gamma \in [0^\circ, 60^\circ]$ , evaluated for a scale factor  $\mathcal{I}_0 = 25 \text{ MeV}^{-1}$ . Right-side: The wobbling frequencies defined in Eq. 17 as function of total angular momentum, evaluated with the parameter set  $\mathcal{P}$  which was obtained through the fitting procedure.

279 moments of inertia of the triaxial core should be indeed consistent with the hydro-  
 280 dynamic model. For the sake of completeness, Figure 3 shows the evolution of a  
 281 hydro-dynamical set of MOIs with respect to the triaxiality parameter  $\gamma$ .

282 Concerning the triaxiality parameter  $\gamma$ , it has a positive value  $\gamma = 22^\circ$ . This  
 283 is consistent with the microscopic descriptions based on cranking mechanism for  
 284 the potential energy surface (PES) of  $^{163}\text{Lu}$  (discussion on PES was done in the  
 285 previous sections). In fact, the agreement is quite good with the predicted deformed  
 286 minima of  $(\beta_2, \gamma) \approx (0.38, 20^\circ)$  [? ?]. Comparing the current W2 model with already  
 287 existing descriptions which take  $\gamma$  to be fixed a-priori throughout the calculations  
 288 (e.g., [? ?]), here  $\gamma$  is obtained through the fitting process in a self-consistent  
 289 manner. Moreover, its value is slightly larger than the one obtained in W1 formalism  
 290 ( $\gamma = 17^\circ$ ). This might be due to the larger ratios  $\mathcal{I}_1/\mathcal{I}_{2,3}$ , which in the present case  
 291 they appear to be bigger ( $\mathcal{I}_1/\mathcal{I}_2 \approx 4.8$  for W2, compared to  $\approx 3.2$  in the previous  
 292 approach W1).

293 Finally, the single-particle potential strength, which causes the odd-proton to  
 294 move in the quadrupole deformed mean-field, has a value of  $V = 2.1 \text{ MeV}$ . In W1, this  
 295 parameter was  $V^{\text{TSD1,2,3}} = 3.1 \text{ MeV}$  and  $V^{\text{TSD4}} = 0.7 \text{ MeV}$ . An explanation for its  
 296 decrease in the present case might be due to the upward shift in the energy caused by  
 297 the un-favored partner, or due to the energetic shift of the parity partner, indicating a  
 298 quenching effect on the quadrupole deformation of the triaxial system. Nevertheless,  
 299 the obtained value seems to be consistent with the previous calculations, the current  
 300 value of  $V$  being close to the average value of  $V$ 's from W1. Other interpretations [?]   
 301 that were developed using a similar single-particle potential term in the Hamiltonian

adopted values of around  $V = 1.6$  MeV, however, that was for an isotope with smaller quadrupole deformation  $\beta_2 = 0.18$ . Interesting research using a single- $j$  shell model which was aimed at obtaining a realistic expression for the deformation parameter has been performed in [? ]. Therein, results for the potential strength of odd- $A$  nuclei with similar mass, but different quasiparticle configurations were numerically obtained. Adoption of an equivalent description for the odd- $j$  particle within W2 could be done, and then compare results for a corresponding configuration. This could be the motivating factor for future work. Concluding this subsection, the obtained values of  $\mathcal{P}$  seem to not only describe the wobbling spectrum of  $^{163}\text{Lu}$  very well (see results in Figures 1 and 2), but they are also consistent with the previous formalism W1, or even with other interpretations from the literature.

#### 4.2. COMMENT ON THE WOBBLING NATURE OF $^{163}\text{Lu}$

It is worthwhile discussing the results obtained regarding the wobbling spectrum of  $^{163}\text{Lu}$ . Indeed, by using a fitting procedure that minimized the  $\chi^2$  function, it was possible to find a parameter set  $\mathcal{P}$  that provides an agreement with the observed experimental data. However, in the current state, there is no clear evidence on whether the formalism W2 predicts a TW or an LW behavior for the nucleus. According to [? ], the wobbling character is given by the coupling of the odd particle which aligns parallel (LW) or perpendicular (TW) to the axis with the largest MOI. But to see this within the measured data, the interpretation of the wobbling energy as it was defined in Eq. ?? must be performed. As such, according to the definition, one has to subtract an energy state within the first excited wobbling band (the one-wobbling-phonon band) from the average of its adjacent energies that belong to the yrast partner. In the present calculations, the first excited state is  $TSD_3$ , with its yrast partner being the band  $TSD_2$ . Following this procedure, both the experimental wobbling energies, as well as the theoretical ones were calculated according to the Eq. ?. The obtained results are plotted in Figure 4.

From the behavior of  $E_{\text{wob}}$  from Figure 4, it can be seen that the theoretical wobbling spectrum is an increasing function of angular momentum  $I$ , suggesting that  $^{163}\text{Lu}$  would have an LW character. This contrasts the current interpretation on which the wobbling energies are decreasing functions with respect to increasing angular momentum. However, within those formalisms [? ], the wobbling energies are obtained from  $TSD_2$  and  $TSD_1$ , since the one-wobbling-phonon band is  $TSD_2$ , in contradistinction to the present W2 model, where the first excited wobbling band is  $TSD_3$ .

Analyzing the experimental data points from Figure 4, a slight increase with spin can also be observed, suggesting as well that the coupling scheme in  $^{163}\text{Lu}$  achieves an LW character. Indeed, from the lower limit of around  $11/2 \hbar$  and up to

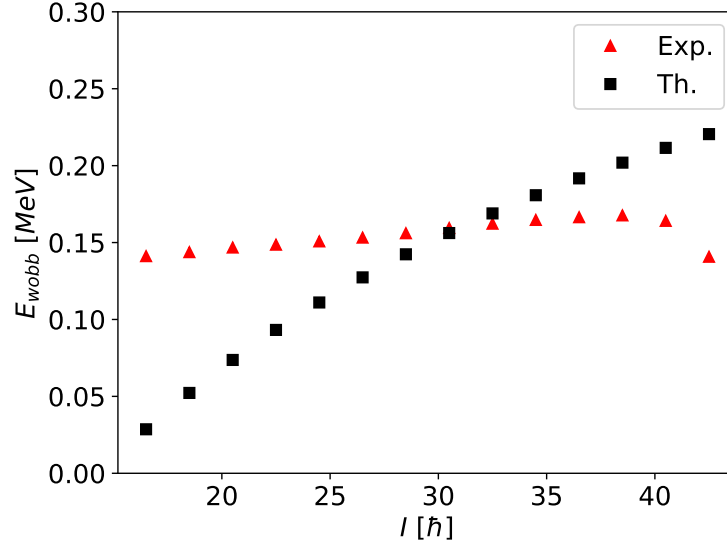


Fig. 4 – The wobbling energies for  $^{163}\text{Lu}$  given as  $E_{\text{wob}} = E_1(I) - \frac{1}{2}(E_0(I+1) + E_0(I-1))$ . According to the current w2 formalism, the sets of energies  $E_1$  belong to  $TSD_3$ , while  $E_0$  correspond to  $TSD_2$ . Experimental data is taken from [? ]. Theoretical values were calculated with the parameter set  $\mathcal{P}$ .

a spin of about  $39/2 \hbar$ , the energy is increasing, then it starts to decrease once  $I \geq 39/2 \hbar$ . The increasing behavior of the theoretical data also appears to be quenched in the high-spin limit, indicating that indeed, once the nucleus reaches high rotational states, a change in the wobbling regime might emerge, and the nucleus can transition from a wobbling regime (LW) to another (TW).

Referring back to the the case of  $^{183}\text{Au}$  [? ], the two observed wobbling bands are based on different alignments: the  $\pi(i_{13/2})$  nucleon (for the so-called *positive parity band*) and the  $\pi(h_{9/2})$  nucleon (for the *negative-parity band*) coupled to a triaxial rotor, respectively. The remarking aspect of this research is that within a PRM model amended with the HFA (harmonic frozen alignment) approximation, it is implied that the configurations of both bands have a transverse (TW) character. However, the wobbling energies  $E_{\text{wob}}$  in these bands have different behavior with respect to the increase of angular momentum. Namely,  $E_{\text{wob}}$  increases (decreases) with spin for the positive (negative) parity configurations (see Figures 3 and 5 from [? ]). This indicates that an increasing/decreasing behavior for  $E_{\text{wob}}$  is not enough evidence for asserting a wobbling character on a triaxial nucleus (at least, not without some strong constraints on the coupling scheme between the core and the odd particle).

Concluding this comment on the wobbling nature for  $^{163}\text{Lu}$ , if the behavior



of the wobbling energies with spin is the sole player in determining the wobbling character of a nucleus, then one could argue that indeed, based on the current results,  $^{163}\text{Lu}$  behaves as a longitudinal wobblers. On the other hand, considering the newly obtained results discussed in the previous paragraphs, the evidence is not enough for making a clear assumption on which type of wobbling motion occurs.

## 5. CONCLUSIONS & OUTLOOK

The purpose of the present work was two-fold. On one hand, a detailed overview regarding the current experimental observations for wobbling motion in both even- and odd-mass nuclei across several mass regions was made in the introductory part (covered in Section ??). This was accompanied by a brief mention of the theoretical methods that are used for the microscopic/macrosopic description of the wobbling phenomenon (see Section ??). Also in the first part of the paper, a schematic analysis on the characteristics of the wobbling motion was made, which concerned the particle-core configurations in a longitudinal/transverse wobblers. Therein, it was shown that depending on the alignment of the odd quasiparticle with the triaxial core, a certain wobbling regime will prevail, thus concluding the introduction.

On the other hand, the second objective of the current paper was to extend a previous model that describes the  $^{163}\text{Lu}$  using a re-interpretation of its four wobbling bands  $TSD_{1,2,3,4}$ . The previous model (denoted here by W1) introduced the concept of signature partners between the bands  $TSD_1$  and  $TSD_2$ . One showed that the nucleus can be described as a particle that is moving in a quadrupole deformed mean field generated by the core. In W1, there was an  $i_{13/2}$  proton involved in the particle-rotor-coupling for the description of the first three triaxial bands, and another proton with negative parity, i.e., the  $\pi(h_{9/2})$  intruder for band  $TSD_4$ . Based on W1, a new approach was developed here as an extension, denoted throughout the paper by W2. The new formalism starts with the same Hamiltonian, however, in the present case a single trial function is constructed to admit eigenstates with both positive and negative parity. Indeed, despite the fact that  $TSD_4$  is of an opposite parity than the first three, all bands are described by the coupling of a unique single-particle ( $i_{13/2}$  with positive parity  $\pi_j = +1$ ) to the core states of positive parity for  $TSD_{1,2,3}$  and core states of negative parity for  $TSD_4$ . The coupling schemes for the wobbling bands within W2 were denoted throughout the paper by  $C'_1, C'_2, C'_3$ . From the quantal Hamiltonian specific to a Particle Rotor Model (given by Eq. 1), by applying a Time-Dependent Variational Principle (TDVE) as in Eq. 6 with the trial function carefully chosen so that it allows a mixture of both positive and negative parity states, a set of analytical expressions for the excitation energies of each band were obtained (defined in Eq. 19). The excitation energies comprise a term that represents the classical

energy function, obtained as the average of the Hamiltonian with the trial wave function (Eq. 21). A second term has a phonon character (Eq. 20), being composed of two wobbling frequencies that were obtained from the solutions to a dispersion-like equation as defined in Eq. 12.

From the theoretical formalism of the excitation energies of  $^{163}\text{Lu}$ , a set of free parameters emerged, containing the three moments of inertia, the single-particle potential strength  $V$ , and the triaxiality parameter  $\gamma$ . They were obtained through a fitting procedure which was done for all four bands, unlike the previous W1 approach. The resulted parameter set provides an impressive agreement between the existing theoretical and experimental data concerning the wobbling spectrum of this isotope, with an r.m.s. of about 79 keV. An interpretation of the numerical values for the obtained parameters was done in Section 4.1, and indeed, the obtained values are consistent with other formalisms from the literature. Furthermore, the study of the classical energy function was done in a polar coordinate system, obtaining the contour plots for spin states belonging to each triaxial band (Section ??). The critical points from those contour maps indicate stability in terms of wobbling behavior (with closed orbits signaling stable trajectories). Unstable regions also emerge at high rotational energies. An additional comment on the wobbling nature of  $^{163}\text{Lu}$  was made (see Section 4.2), and an analysis of the wobbling energy behavior with spin showed that the increasing trend might indicate a longitudinal character. Lastly, by intersecting the angular momentum sphere with the energy ellipsoid, the classical trajectories can be obtained. The results of this 3-dimensional representation are discussed throughout Section ??.

From the graphical illustrations, three situations might occur for any given spin state of  $^{163}\text{Lu}$ . i) At low energies, the rotation axis is either the 1-axis or the  $-1$ -axis, resulting in two trajectories along this axis. ii) At a particular energy - *critical energy* - the two orbits get close to each other until they intersect, marking the point of unstable motion for the nucleus. iii) If the energy increases even more, then the triaxial nucleus performs a tilted-axis-rotation, where the rotational axis slowly moves away from  $x_1$ , approaching  $x_3$  and thus becoming misaligned. The change from one step to the other marks a phase transition. When the nucleus undergoes a transformation with regards to its rotational behavior it is actually changing its wobbling regime. Remarkable the fact that the current semi-classical approach is able to predict the change in the wobbling regime, this being of large interest in the nuclear community since evidence of such behavior was missing.

Concluding the present work, this newly developed formalism proves to be a successful tool for accurately describing the wobbling spectrum of  $^{163}\text{Lu}$  and also for providing an insight into the rotational motion of the nuclear system with respect to its total spin.

*Acknowledgments.* This work was supported by UEFISCU, through the project **PCE-16/2021**.

Table 4

This table is taken from RJP volume **50**(1-2) from page 43 (2005). It gives the “*number of bound states dependence on the radius of space curvature for  $\alpha = 0.005$ ,  $U_0 = 1$* ”.

Value $\rho$	Value $\varepsilon$
$\rho = 50$	–
$\rho = 100$	–
$\rho = 250$	$\varepsilon_1 = 0.0289$
$\rho = 400$	$\varepsilon_1 = 0.3772$
$\rho = 1000$	$\varepsilon_1 = 0.4142, \varepsilon_2 = 0.8495$

## REFERENCES

1. D. E. Knuth, D. R. Bibby, “*The TeXbook*”, 20th edn. (AMS & Addison-Wesley Publ. Co., 1991).
2. D. E. Knuth homepage: [www-cs-faculty.stanford.edu/~knuth](http://www-cs-faculty.stanford.edu/~knuth).